6-2010

5 GHz Band Vehicle-to-Vehicle Channels: Models for Multiple Values of Channel Bandwidth

Qiong Wu

David W. Matolak
University of South Carolina - Columbia, matolak@cec.sc.edu

Indranil Sen

Publication Info

Postprint version. Published in *IEEE Transactions on Vehicular Technology*, Volume 59, Issue 5, 2010, pages 2620-2625.

Wu, Q., Matolak, D., Sen, I. (2010). 5 GHz Band Vehicle-to-Vehicle Channels: Models for Multiple Values of Channel Bandwidth. *IEEE Transactions on Vehicular Technology, 59(5)*, 2620-2625.
http://dx.doi.org/10.1109/TVT.2010.2043455

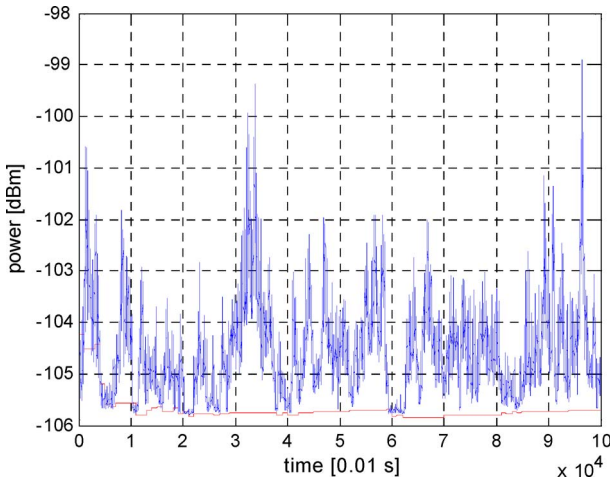

Fig. 5. (Blue) Measured RTWP and (red) estimated noise power floor.

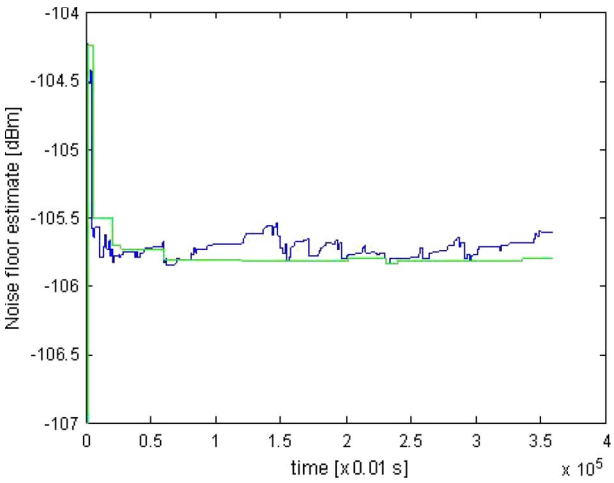

Fig. 6. Comparison between the sliding-window algorithm (green) and the proposed recursive algorithm.

These are dominated by the recursive noise floor estimator. The states are given by the $2M$ scalars $f_{\min\{x^{n+\text{thermal}}(t'),t'\in\bar{I}_r\}|\mathbf{Y}^{t_r}}(t_r,x_m)$, $m=0,\ldots,M$ and $\Gamma(t_r,x_m)$, $m=0,\ldots,M$. The setting used here results in a need to store 1000 state variables for each instance of the algorithm. With 100 instances of the algorithm in an RBS, a memory consumption of 800 kB results, assuming double-precision arithmetics. The sliding-window algorithm, on the contrary, needs to store power quantities of the same size as the state variable of the recursive algorithm $2M$ but *for each power sample in the sliding window*. Since the window contains about 100 such power samples, a memory consumption of 80 MB would result.

VI. Conclusion

The noise-floor-estimation problem in the WCDMA uplink has been discussed, and a new recursive noise-floor-estimation algorithm has been presented. The algorithm enhances the thermal noise power noise floor tracking ability to a dynamic range of many tens of decibels. The recursive algorithm also dramatically reduces the memory requirements, as compared with previous sliding-window algorithms, thereby enabling implementation of multiple instances of the algorithm running in parallel in the RBS.

Acknowledgment

The author would like to thank his employer Ericsson AB, in particular M.Sc. E. Schön, for the permission to publish this paper.

References

[1] FDD Enhanced Uplink; Overall description; Stage 2, Jun. 2005, 3GPP TS 25.309, rel. 6 (v6.3.0). [Online]. Available: http://www.3gpp.org/ftp/Specs/html-info/25309.htm

[2] H. Holma and A. Toskala, *WCDMA for UMTS—Radio Access for Third Generation Mobile Communications*. Chichester, U.K.: Wiley, 2000.

[3] J. Zander, "Transmitter power control for co-channel interference management in cellular radio systems," in *Proc. WINLAB Workshop*, New Brunnswick, NJ, 1993, pp. 241–247.

[4] E. G. Lundin, P. Karlsson, and S. Craig, "Interference power based uplink admission control in enhanced WCDMA," in *Proc. IEEE Veh. Technol. Conf.*, Baltimore, MD, Oct. 1–3, 2007, pp. 1726–1730.

[5] Requirements for support of radio resource management (FDD), Sep. 2009, 3GPP TS 25.133, release 8 (v. 8.4.0). [Online]. Available: http://www.3gpp.org/ftp/Specs/html-info/25133.htm

[6] T. Wigren, "Soft uplink load estimation in WCDMA," *IEEE Trans. Veh. Technol.*, vol. 58, no. 2, pp. 760–772, Mar. 2009.

[7] T. Wigren and P. Hellqvist, "Estimation of uplink WCDMA load in a single RBS," in *Proc. IEEE Veh. Technol. Conf.*, Baltimore, MD, Oct. 1–3, 2007, pp. 1499–1503.

[8] T. Söderström, *Discrete-Time Stochastic Systems—Estimation and Control*. Hemel Hempstead, U.K.: Prentice-Hall, 1994.

5-GHz-Band Vehicle-to-Vehicle Channels: Models for Multiple Values of Channel Bandwidth

Qiong Wu, David W. Matolak, *Senior Member, IEEE*, and Indranil Sen

***Abstract*—In Sen and Matolak's earlier paper, 5-GHz-band vehicle-to-vehicle (V2V) channel models were presented for channel bandwidths of 5 and 10 MHz. In this paper, we provide additional tapped delay line models for bandwidths of 1, 20, 33.33, and 50 MHz based upon the data used in Sen and Matolak's paper. We provide tables of channel parameters for five types of V2V channel classes and also include example tap correlation coefficients. Root-mean-square delay spread values are summarized, as are values of bandwidth for which the channel frequency correlation takes values of 0.7 and 0.5. As with the results from Sen and Matolak's paper, these models should be useful for designers in future V2V communication systems.**

***Index Terms*—Channel impulse response, fading, radio propagation.**

I. Introduction

During the past decade, research related to vehicle-to-vehicle (V2V) communication has steadily been growing, e.g., [1] and [2]. Numerous applications within the area of intelligent transportation systems are being proposed and investigated. As in other types of wireless

Manuscript received August 31, 2009; revised November 13, 2009, January 12, 2010, and February 4, 2010; accepted February 5, 2010. Date of publication February 22, 2010; date of current version June 16, 2010. The review of this paper was coordinated by Prof. M. D. Yacoub.

Q. Wu and D. W. Matolak are with the School of Electrical Engineering and Computer Science, Ohio University, Athens, OH 45701 USA (e-mail: qw208706@ohio.edu; matolak@ohio.edu).

I. Sen was with the School of Electrical Engineering and Computer Science, Ohio University, Athens, OH 45701 USA. He is now with Apple Computer Inc., Cupertino, CA 95014 USA (e-mail: indranil.sen@gmail.com).

Digital Object Identifier 10.1109/TVT.2010.2043455

TABLE I
CHANNEL PARAMETERS FOR 1-MHz-BANDWIDTH V2V CHANNELS (MODEL-1)

Tap Index k	Energy	Weibull Factor (β_k)	$P_{00,k}$	$P_{11,k}$	P_1
UOC					
1	0.9650	2.97	na	1.0000	1.0000
2	0.0350	0.40	0.7635	0.7614	0.4978
Small City					
1	0.9763	3.99	na	1.0000	1.0000
2	0.0237	1.58	0.8238	0.5699	0.2897
OHT					
1	0.9634	4.56	na	1.0000	1.0000
2	0.0366	1.51	0.6815	0.7683	0.5792
OLT					
1	0.9706	5.30	na	1.0000	1.0000
2	0.0294	1.51	0.6814	0.7757	0.5864
UIC					
1	0.9145	2.40	na	1.0000	1.0000
2	0.0855	1.61	0.4639	0.8311	0.7608

TABLE II
CHANNEL PARAMETERS FOR 20-MHz-BANDWIDTH V2V CHANNELS (MODEL-1)

Tap Index k	Energy	Weibull Factor (β_k)	$P_{00,k}$	$P_{11,k}$	P_1
UOC					
1	0.8090	3.17	na	1.0000	1.0000
2	0.0882	1.69	0.2523	0.9287	0.9129
3	0.0398	1.70	0.3538	0.8615	0.8236
4	0.0237	1.69	0.4919	0.7911	0.7088
5	0.0162	1.68	0.5768	0.7172	0.5995
6	0.0132	1.71	0.6219	0.7176	0.5724
7	0.0100	1.74	0.6719	0.6732	0.5012
Small City					
1	0.8111	4.11	na	1.0000	1.0000
2	0.1033	2.00	0.1364	0.9396	0.9315
3	0.0513	1.72	0.375	0.8897	0.8505
4	0.0230	2.00	0.3790	0.7378	0.7041
5	0.0113	2.24	0.5091	0.7476	0.6573
OHT					
1	0.9073	4.49	na	1.0000	1.0000
2	0.0642	1.64	0.2239	0.8853	0.8713
3	0.0178	2.00	0.5188	0.7330	0.6429
4	0.0107	2.00	0.6084	0.6161	0.5048
OLT					
1	0.9196	4.97	na	1.0000	1.0000
2	0.0635	1.63	0.2293	0.8839	0.8693
3	0.0170	1.69	0.5057	0.7145	0.6344
UIC					
1	0.6498	2.73	na	1.0000	1.0000
2	0.1109	1.75	0.0952	0.9717	0.9697
3	0.0619	1.79	0.1800	0.9362	0.9280
4	0.0381	1.79	0.3486	0.8784	0.8429
5	0.0284	2.00	0.3986	0.8367	0.7867
6	0.0238	2.00	0.4885	0.8304	0.7493
7	0.0218	1.79	0.4219	0.7804	0.7233
8	0.0178	1.76	0.5221	0.7687	0.6744
9	0.0132	1.59	0.5933	0.6921	0.5677
10	0.0114	1.77	0.6767	0.7072	0.5231
11	0.0093	1.59	0.6963	0.6302	0.4496
12	0.0079	2.00	0.6939	0.6338	0.4539
13	0.0056	2.00	0.7512	0.6030	0.3862

communication systems, accurate models of the wireless channel are vital to system design and performance evaluation. We refer the reader to [1] for a thorough discussion of background on V2V applications, frequency bands, and more detail on related work, some of which have been for narrowband V2V channel models.

TABLE III
CHANNEL PARAMETERS FOR 33.33-MHz-BANDWIDTH V2V CHANNELS (MODEL-1)

Tap Index k	Energy	Weibull Factor (β_k)	$P_{00,k}$	$P_{11,k}$	P_1
UOC					
1	0.7858	3.26	Na	1.0000	1.0000
2	0.0804	1.68	0.2707	0.9233	0.9048
3	0.0394	1.73	0.3744	0.8727	0.8309
4	0.0270	1.67	0.4405	0.83	0.7670
5	0.0178	1.77	0.5419	0.7686	0.6646
6	0.0142	1.71	0.6200	0.7242	0.5796
7	0.0114	1.71	0.6251	0.6856	0.5440
8	0.0092	1.68	0.7038	0.6563	0.4630
9	0.0075	1.76	0.7116	0.6318	0.4394
10	0.0073	2.00	0.7283	0.6214	0.4180
Small City					
1	0.7608	4.53	na	1.0000	1.0000
2	0.0987	2.17	0.0833	0.9643	0.9626
3	0.0638	2.00	0.1	0.9069	0.9065
4	0.0378	1.77	0.24	0.8593	0.8442
5	0.0181	2.00	0.2976	0.7542	0.7383
6	0.0116	2.00	0.4874	0.6965	0.6293
7	0.0097	2.17	0.4833	0.695	0.6262
OHT					
1	0.8910	4.40	na	1.0000	1.0000
2	0.0684	1.54	0.2465	0.8994	0.8820
3	0.0210	1.68	0.4417	0.7874	0.7244
4	0.0111	1.57	0.6392	0.6258	0.4908
5	0.0085	1.62	0.6407	0.5868	0.465
OLT					
1	0.9013	5.29	na	1.0000	1.0000
2	0.0681	1.27	0.2857	0.8902	0.8668
3	0.0190	1.61	0.4468	0.7839	0.7196
4	0.0116	1.66	0.6384	0.6246	0.4913
UIC					
1	0.5991	2.69	na	1.0000	1.0000
2	0.1068	1.76	0.1333	0.9808	0.9784
3	0.0621	2.00	0.1373	0.9315	0.9265
4	0.0405	1.71	0.2841	0.8959	0.8732
5	0.0289	1.74	0.3739	0.8754	0.8343
6	0.0221	1.73	0.3605	0.8278	0.7882
7	0.0204	2.00	0.425	0.7647	0.7104
8	0.0175	2.00	0.5405	0.7834	0.6801
9	0.0143	2.00	0.4623	0.7651	0.6945
10	0.0145	1.67	0.5126	0.7451	0.6571
11	0.0113	2.00	0.5434	0.7196	0.6182
12	0.0112	2.00	0.5668	0.7115	0.6009
13	0.0100	2.00	0.5942	0.6753	0.5562
14	0.0092	1.56	0.6503	0.6513	0.5
15	0.0070	1.66	0.6967	0.6151	0.4395
16	0.0077	1.68	0.6992	0.6401	0.4539
17	0.0061	2.00	0.7063	0.5730	0.4063
18	0.0064	1.57	0.7512	0.5970	0.3804
19	0.0049	1.74	0.7397	0.5569	0.3689

In addition to the related work cited in [1], wideband measurements made for expressway channels in the 2- and 5-GHz bands were reported in [3] and [4]. In [3], the authors reported an eight-tap channel model for a bandwidth of 10 MHz, whereas in [4], the authors proposed six- and 12-tap channel models for a bandwidth of 20 MHz. Another band that is being planned for use in V2V communication is the 5.9-GHz dedicated short-range communication (DSRC) band. For DSRC, the available bandwidth is 75 MHz, and this is divided into seven 10-MHz channels.

Additional recent empirical work on V2V channels includes path loss at 2.1 GHz in [5], 5.2-GHz band delay spread comparisons among two measurement campaigns [6], 5.9-GHz band delay and Doppler spread results in [7], nonstationary scattering function results at

TABLE IV
CHANNEL PARAMETERS FOR 50-MHz-BANDWIDTH V2V CHANNELS (MODEL-1)

Tap Index k	Energy	Weibull Factor (β_k)	$P_{00,k}$	$P_{11,k}$	P_1
UOC					
1	0.7193	3.40	Na	1.0000	1.0000
2	0.1115	1.66	0.2534	0.9539	0.9418
3	0.0378	1.76	0.3279	0.8973	0.8675
4	0.0295	2.00	0.3246	0.8732	0.8419
5	0.0234	1.70	0.4009	0.8269	0.7759
6	0.0162	2.00	0.4317	0.7841	0.7247
7	0.0127	2.00	0.5213	0.747	0.6544
8	0.0117	1.79	0.6041	0.7014	0.5702
9	0.0085	1.73	0.6692	0.6685	0.4994
10	0.0080	2.00	0.6299	0.6654	0.5254
11	0.0067	2.00	0.7246	0.6184	0.4194
12	0.0056	2.00	0.6996	0.5994	0.4286
13	0.0050	2.00	0.7524	0.5937	0.3789
14	0.0047	2.00	0.7233	0.5872	0.4015
Small City					
1	0.6739	6.09	na	1.0000	1.0000
2	0.1319	2.00	0	0.9711	0.9720
3	0.0595	2.00	0	0.9298	0.9346
4	0.0453	2.00	0.1212	0.8990	0.8972
5	0.0298	2.00	0.1463	0.8746	0.8723
6	0.0221	1.76	0.2623	0.8263	0.8100
7	0.0142	2.00	0.25	0.7705	0.7632
8	0.0089	2.18	0.4783	0.7122	0.6417
9	0.0070	2.51	0.475	0.685	0.6262
10	0.0073	2.25	0.519	0.6487	0.5763
OHT					
1	0.8296	4.65	na	1.0000	1.0000
2	0.1052	1.38	0.2437	0.9474	0.9347
3	0.0274	1.48	0.2644	0.8728	0.8526
4	0.0153	1.77	0.45	0.7738	0.7088
5	0.0096	1.23	0.5757	0.6564	0.5523
6	0.0073	1.40	0.6114	0.5908	0.4872
7	0.0056	2.00	0.6694	0.5518	0.4244
OLT					
1	0.8453	5.41	na	1.0000	1.0000
2	0.106	1.44	0.1143	0.9455	0.9421
3	0.0257	1.38	0.2791	0.8803	0.8577
4	0.0140	1.69	0.3419	0.7305	0.7097
	0.0090	1.77	0.5515	0.6199	0.5418
UIC					
1	0.5364	2.71	na	1.0000	1.0000
2	0.1114	2.00	0.0556	0.9748	0.9741
3	0.0678	1.71	0.125	0.9576	0.9539
4	0.0438	2.00	0.1404	0.9230	0.9179
5	0.0337	1.76	0.3585	0.8842	0.8473
6	0.0267	2.00	0.2768	0.8606	0.8386
7	0.0176	2.00	0.3636	0.8346	0.7940
8	0.0170	2.00	0.4207	0.8185	0.7623
9	0.0134	2.00	0.4677	0.7825	0.7104
10	0.0123	2.00	0.4492	0.7155	0.6599
11	0.0115	2.00	0.5154	0.7640	0.6729
12	0.0100	2.00	0.5311	0.6976	0.6066
13	0.0093	2.00	0.5166	0.6896	0.6095
14	0.0096	2.00	0.5533	0.6791	0.5807
15	0.0099	2.00	0.6027	0.7046	0.5721
16	0.0077	2.12	0.6026	0.6839	0.5576
17	0.0071	2.00	0.6232	0.6461	0.5144
18	0.0073	2.01	0.6330	0.6749	0.5288
19	0.0062	2.00	0.6419	0.6061	0.4755
20	0.0067	1.73	0.6729	0.6120	0.4582
21	0.0055	1.75	0.7327	0.6263	0.4179
22	0.0051	2.00	0.7146	0.6069	0.4193
23	0.0047	2.08	0.7167	0.5678	0.3948
24	0.0046	2.00	0.7171	0.5936	0.4092
25	0.0037	2.00	0.7517	0.5413	0.3501
26	0.0040	2.00	0.7747	0.5419	0.3285
27	0.0035	2.00	0.7979	0.5785	0.3228
28	0.0034	2.00	0.7743	0.5160	0.317

TABLE V
CHANNEL PARAMETERS FOR MODEL-2 20-MHz UOC V2V CHANNEL

Tap Index k	Energy	Weibull Factor (β_k)	$P_{00,k}$	$P_{11,k}$	P_1
1	0.7777	3.17	na	1.0000	1.0000
2	0.0848	1.69	0.2528	0.9287	0.9129
3	0.0382	1.70	0.3538	0.8615	0.8236
4	0.0228	1.69	0.4919	0.7911	0.7088
5	0.0156	1.68	0.5768	0.7172	0.5995
6	0.0126	1.71	0.6219	0.7176	0.5724
7	0.0097	1.74	0.6719	0.6732	0.5012
8	0.0069	1.75	0.7349	0.6059	0.4021
9	0.0050	1.79	0.7797	0.5603	0.3341
10	0.0034	1.74	0.8113	0.4931	0.2715
11	0.0028	2.00	0.8469	0.4966	0.2332
12	0.0023	1.73	0.8873	0.4807	0.1783
13	0.0019	1.64	0.8956	0.4120	0.1508
14	0.0015	2.00	0.9178	0.4460	0.1292
15	0.0013	1.49	0.9353	0.4207	0.1005
16	0.0011	1.29	0.9418	0.3698	0.0845
17	0.0010	1.22	0.9548	0.3944	0.0698
18	0.0012	1.31	0.9595	0.4810	0.0724
19	0.0010	1.23	0.9554	0.4488	0.0749
20	0.0011	1.36	0.9554	0.4073	0.0700
21	0.0011	1.23	0.9655	0.4426	0.0582
22	0.0007	1.06	0.9692	0.3843	0.0476
23	0.0011	0.94	0.9701	0.4586	0.0523
24	0.0027	0.80	0.9739	0.5704	0.0572
25	0.0004	1.06	0.9770	0.3757	0.0356
26	0.0004	1.05	0.9774	0.3729	0.0348
27	0.0004	0.91	0.9772	0.3488	0.0338
28	0.0004	0.99	0.9811	0.4364	0.0324
29	0.0005	0.93	0.9824	0.4082	0.0289
30	0.0005	1.07	0.9821	0.4854	0.0336

5.2 GHz in [8], multiple-input/multiple-output correlation results at 5.2 GHz in [9], and our own work on nonstationary Markov modeling in [10]. Other than our Markov models in [10] and the ten-tap model in [6], we have found only one other reference that actually provides wideband models that system designers can use, i.e., [11]. This paper provides a 20-MHz highway model for the 5.3-GHz band and also cites severe (worse than Rayleigh) fading for some of the multipath components.

Based upon these results and the DSRC standard, we initially considered channel bandwidths less than or equal to 10 MHz in [1] (5- and 10-MHz V2V models). Due to the ever increasing demands for high-data-rate applications and the increasing numbers of users, future communication systems may require larger bandwidths [12], and so here we present additional channel models for bandwidths of 20, 33.33, and 50 MHz, as these values may be used for next-generation V2V communication systems. We also include models for the small bandwidth value of 1 MHz, since it is possible that this channel bandwidth will be used in some cases—for example, Third Generation Partnership Project's Long Term Evolution allows for a minimum bandwidth value of 1.4 MHz, and some third-generation cellular standards also have bandwidths on the order of 1 MHz. The channel models presented here can be viewed as companions to the 5- and 10-MHz models presented in [1]; hence, this paper constitutes an extension of that work.

Note that these models are empirical based upon measurements and do not presume any general or specific characteristics of the V2V environment, as do so-called "geometric models," e.g., [13]–[16]. In addition, they represent single-input/single-output channels. Although the "geometric models" can be used to accurately model a wide variety of environments, they are often complex and require numerous parameter selections for the specific environment of interest. In

TABLE VI
SUMMARY OF RMS-DS VALUES FOR FIVE V2V REGIONS

Region	RMS-DS (ns) [Min; Mean; Max]			
	1 MHz	20 MHz	33.33 MHz	50 MHz
UIC	[0.2; 294.9; 994.2]	[5.7; 258.3; 1381]	[6.2; 263; 1376.2]	[13.9; 267.7; 1387]
UOC	[0.03; 138.4; 977]	[0.5; 140.9; 1414]	[1; 139.8; 1429.6]	[3.5; 148.6; 1466]
OLT	[0.06; 106.8; 500]	[0.6; 58.8; 1341.3]	[0.8; 56.5; 1408.0]	[3.9; 53.4; 1452.1]
OHT	[0.08; 149.6; 1066]	[1.9; 143.7; 2062]	[1.7; 138.8; 2024]	[3.5; 135.8; 2085]
Small	[0.1; 98.9; 942.2]	[7.6; 181; 2068.4]	[7.2; 160.4; 2152]	[14; 174.6; 2226.3]

TABLE VII
TAP CORRELATION MATRICES FOR 1- AND 20-MHz CHANNELS FOR FIVE V2V REGIONS LOWER TRIANGULAR PART FOR 20 MHz, UPPER TRIANGULAR PART FOR 1 MHz

UIC	**1**	**2**	**3**	**4**	**5**	**6**	**7**	**8**	**9**	**10**	**11**	**12**	**13**
1	1.00	0.6084	NA	NA	NA	NA	NA	NA	NA	NA	NA	NA	NA
2	0.4912	1.00	NA	NA	NA	NA	NA	NA	NA	NA	NA	NA	NA
3	0.4092	0.6123	1.00	NA	NA	NA	NA	NA	NA	NA	NA	NA	NA
4	0.1985	0.2748	0.1926	1.00	NA	NA	NA	NA	NA	NA	NA	NA	NA
5	0.4001	0.4609	0.2125	0.2882	1.00	NA	NA	NA	NA	NA	NA	NA	NA
6	0.4606	0.3892	0.4107	0.4756	0.3511	1.00	NA	NA	NA	NA	NA	NA	NA
7	0.4175	0.3939	0.3349	0.4966	0.4330	0.7389	1.00	NA	NA	NA	NA	NA	NA
8	0.4831	0.4103	0.4594	0.6039	0.2434	0.6596	0.6879	1.00	NA	NA	NA	NA	NA
9	0.7839	0.6950	0.6861	0.3334	0.6564	0.8743	0.8358	0.6584	1.00	NA	NA	NA	NA
10	0.5742	0.5803	0.4253	0.7805	0.2575	0.8532	0.7254	0.9515	0.5728	1.00	NA	NA	NA
11	0.5523	0.6109	0.6708	0.4321	0.3191	0.6604	0.5424	0.6376	0.6907	0.7971	1.00	NA	NA
12	0.8733	0.7672	0.5192	0.4143	0.4677	0.5044	0.5454	0.5853	0.6141	0.6025	0.7226	1.00	NA
13	0.6048	0.3165	0.3329	0.7828	0.5224	0.3975	0.6950	0.7429	0.3585	0.9022	0.2732	0.7445	1.0000
UOC	**1**	**2**	**3**	**4**	**5**	**6**	**7**						
1	1.00	0.6877	NA	NA	NA	NA	NA						
2	0.8656	1.00	NA	NA	NA	NA	NA						
3	0.5997	0.6223	1.00	NA	NA	NA	NA						
4	0.6390	0.8383	0.5055	1.00	NA	NA	NA						
5	0.6147	0.6168	0.6868	0.5213	1.00	NA	NA						
6	0.5926	0.5375	0.8609	0.4999	0.5273	1.00	NA						
7	0.5561	0.3619	0.4928	0.3832	0.5903	0.6766	1.00						
OLT	**1**	**2**	**3**										
1	1.00	0.5149	NA										
2	0.1399	1.00	NA										
3	0.0955	0.2142	1.00										
OHT	**1**	**2**	**3**	**4**									
1	1.00	0.5867	NA	NA									
2	0.7286	1.00	NA	NA									
3	0.7604	0.5618	1.00	NA									
4	0.7253	0.5309	0.8378	1.00									
Small	**1**	**2**	**3**	**4**	**5**								
1	1.00	0.3368	NA	NA	NA								
2	0.8472	1.00	NA	NA	NA								
3	0.0120	0.7503	1.00	NA	NA								
4	0.1017	0.1425	0.1492	1.00	NA								
5	0.2986	0.5370	0.6286	0.1257	1.00								

addition, conventional tapped delay line models are still widely used; hence, the tapped delay line models we provide here can immediately be used by many researchers without requiring them to develop specific geometric models.

II. Results

A. Measurement Summary

As described in detail in [1], for our measurements, we used a 50-MHz bandwidth in the 5-GHz band and combined channel impulse response samples to form models for smaller bandwidths. The measurements reported in [1] were made with a spread-spectrum-stepped correlator with chip rate of 50 MHz and an unambiguous delay range of 5 μs. The antennas were mounted on the vehicle roofs (except one model class for which the antennas were inside the vehicles), and the transmit and receive vehicles moved throughout several environments, e.g., large cities, small cities, and highways in Ohio. The vehicle velocities were limited to near 10 m/s in cities, with intervehicle distances from a few meters to approximately 100 m. Both heavy and light vehicle traffic were encountered, with occasional blockage of the line of sight (LOS) signal by large vehicles (e.g., trucks) and by buildings when the leading vehicle turned a corner, creating non-LOS conditions. The city areas we traversed were those with tall buildings (four to five stories for small cities and more than ten stories for large cities) on both sides of the street. The highway velocities were approximately 26 m/s, with substantially less relative velocities between the vehicles. The intervehicle distances on the highways were up to approximately 1 km, but most data were collected with intervehicle distances between a few tens to several hundred meters. In all environments, measurements were taken with the receiver vehicle both in front of and behind the transmitter vehicle. In [1], we classified the measurement environments into the following five classes: 1) Urban–Antenna Outside Car (UOC); 2) Urban–Antenna Inside Car (UIC); 3) Small City (S); 4) Open Area–Low Traffic Density (OLT); and 5) Open Area High Traffic Density (OHT). The "open" areas are the highways. These region classifications were initially developed in [17].

B. Models

Similar to [1], our results are in the form of tables of V2V channel models for bandwidths of 1, 20, 33.33, and 50 MHz. This should enable the construction of tapped delay line models for analysis, simulations, and potential experiments. We present here what we term "Model-1" [1] parameters for five V2V regions in Tables I–IV. As discussed in [1], Model-1-type channel models have a (slightly) reduced number of taps based on accounting for only 99% of the impulse response cumulative energy. Examples of Model-2-type channel parameters for a 20-MHz UOC region are also provided in Table V. These Model-2-type models employ all taps resolvable with a given bandwidth, with no truncation based upon cumulative energy. The tables contain, for each tap (spaced in delay by the reciprocal of the channel bandwidth), the amplitude fading model parameter, the tap relative energy, and the tap's Markov probability parameters; these are explained next.

Amplitude fading of all taps is modeled using the Weibull probability density function [18], which is equal to the Rayleigh distribution when the Weibull β parameter is 2. As Tables I–V show, worse than Rayleigh fading ($\beta < 2$, as also found in [19]) occurs on a number of channel taps. Explanations for such "severe" fading include invalidation of the central limit theorem due to an insufficiently large number of unresolvable multipath components per delay bin, multiple scattering [20], and frequent channel transitions [21], which redistribute the multipath energy among components, resulting in a given component having worse than Rayleigh fading. Note also that this severe fading could be modeled via the $\alpha-\mu$ distribution [22], which can even account for the most severe cases, e.g., the latter half of the taps in the 20-MHz UOC model of Table V, corresponding to cases in which the Nakagami parameter m is smaller than 0.5 (β smaller than 1.44).

We also continue the use of first-order homogeneous Markov tap persistence processes, which essentially "switch" taps "on" and "off," and hence these processes model the finite lifetime associated with multipath components. Details regarding the Markov models appear in [1], along with posited physical explanations for this phenomenon—rapid obstructions by other vehicles or buildings and possibly, as noted in [13] and [23], drift of multipath components into other delay bins. Here, we include the Markov steady-state and transition probabilities within the tapped delay line model tables. The steady-state probabilities are the probability of the tap being "on" (above our 25-dB threshold from the strongest tap) (P_1) or "off" $(P_0 = 1 - P_1)$. The transition probabilities denote the probabilities of switching between these states, e.g., $P_{00} = Pr(off \rightarrow off)$ in one time step. The transition probabilities satisfy $P_{00} = 1 - P_{01}$ and $P_{11} = 1 - P_{10}$. As noted in [1], the longer delay taps do not persist as long as the shorter delay taps.

Table VI summarizes the root-mean square delay spread (RMS-DS) values for these V2V regions. Table VII contains example correlation coefficients among taps for the different regions for Model-1-type models for the 1- and 20-MHz bandwidths. Since the correlation coefficient matrix is symmetric, for compactness of presentation, the lower and upper triangular parts of the matrices in these tables correspond to correlations for different model bandwidths or different V2V regions. The bandwidths (in megahertz) for which the frequency correlation estimates (FCEs) [24] take values of 0.7 for the vector of channel classes [UIC, UOC, OHT, OLT, S] are as follows: 1 MHz [NA, 0.62, 0.59, 0.57, NA]; 20 MHz [5.8, 7.0, 7.5, 7.7, 7.2]; 33.33 MHz [10.1, 10.8, 10.8, 12.6, 9.9]; and 50 MHz [6.8, 7.7, 8.3, 9.0, 8.3]. The analogous bandwidth values for correlation level 0.5 are as follows: 1 MHz [NA, NA, NA, 0.86, NA]; 20 MHz [9.9, 10.5, 10.8, 11.1, 11.1]; 33 MHz [18.4, 16.8, 15.7, 18.4, 14.6]; and 50 MHz [11.6, 11.5, 12.0, 12.7, 11.8]. The bandwidth values cited are the smallest frequency separations for which the FCE attains the correlation value.

III. Conclusion

In this paper, we have provided empirical V2V channel models for the 5-GHz band in the form of tapped delay line specifications. These models are for bandwidth values of 1, 20, 33.33, and 50 MHz and augment the models provided in [1] for channel bandwidths of 5 MHz and 10 MHz. The models employed the same measured data set as in [1] for multiple V2V environments, including large cities, small cities, and highways. These models should be of use to V2V communication system researchers and designers.

References

[1] I. Sen and D. W. Matolak, "Vehicle–vehicle channel models for the 5-GHz band," *IEEE Trans. Intell. Transp. Syst.*, vol. 9, no. 2, pp. 235–245, Jun. 2008.

[2] ITS Project Website, Feb. 2007. [Online]. Available: http://www.its.dot.gov/index.htm

[3] G. Acosta-Marum and M. Ingram, "Doubly selective vehicle-to-vehicle channel measurements and modeling at 5.9 GHz," in *Proc. Wireless Personal Multimed. Commun. Conf.*, San Diego, CA, Sep. 13–16, 2006, pp. 143–148.

[4] G. Acosta-Marum and M. Ingram, "Model development for the wideband vehicle-to-vehicle 2.4 GHz channel," in *Proc. Wireless Commun. Netw. Conf.*, Apr. 3–6, 2006, vol. 3, pp. 1283–1288.

[5] K. Konstantinou, S. Kang, and C. Tzaras, "A measurement based model for mobile-to-mobile UMTS links," in *Proc. IEEE Veh. Technol. Conf.*, Singapore, May 11–14, 2008, pp. 529–533.
[6] A. Paier, J. Karedal, N. Czink, C. Dumard, T. Zemen, F. Tufvesson, C. F. Meclenbrauker, and A. F. Molisch, "Comparison of Lund'07 vehicular channel measurements with the IEEE 802.11p model," in *Proc. COST 2100*, Wroclaw, Poland, Feb. 6–8, 2008.
[7] P. Paschalidis, M. Wisotzki, A. Kortke, M. Peter, and W. Keusgen, "Wideband car-to-car MIMO radio channel measurements at 5.7 GHz and issues concerning application-oriented systems," in *Proc. 1st IEEE Veh. Technol. Soc. WAVE Conf.*, Dearborn, MI, Dec. 8–9, 2008. [CD-ROM].
[8] A. Paier, T. Zemen, L. Bernado, G. Matz, J. Karedal, N. Czink, C. Dumard, F. Tufvesson, A. Molisch, F. Mecklenbrauker, and F. Christoph, "Non-WSSUS vehicular channel characterization in highway and urban scenarios at 5.2 GHz using the local scattering function," in *Proc. Int. Workshop Smart Antennas*, Darmstadt, Germany, Feb. 26–27, 2008, pp. 9–15.
[9] A. Paier, T. Zemen, J. Karedal, N. Czink, C. Dumard, F. Tufvesson, C. F. Mecklenbrauker, and A. F. Molisch, "Spatial diversity and spatial correlation evaluation of measured vehicle-to-vehicle radio channels at 5.2 GHz," in *Proc. IEEE Radio Wireless Symp.*, San Diego, CA, Jan. 18–22, 2009, pp. 326–330.
[10] D. W. Matolak and Q. Wu, "Markov models for vehicle-to-vehicle channel multipath persistence processes," in *Proc. 1st IEEE Veh. Technol. Soc. WAVE Conf.*, Dearborn, MI, Dec. 8–9, 2008. [CD-ROM].
[11] O. Renaudin, V.-M. Kolmonen, P. Vainikainen, and C. Oestges, "Car-to-car channel models based on wideband MIMO measurements at 5.3 GHz," in *Proc. 3rd Eur. Conf. Antennas Propag.*, Berlin, Germany, Mar. 23–27, 2009.
[12] R. Roy, DSRC and ISO CALM-M5 V2V standards groups, personal communication, Aug. 2008. [Online]. Available: http://www.iso.org/iso/iso_catalogue/catalogue_tc/catalogue_detail.htm?csnumber=51398
[13] J. Karedal, F. Tufvesson, N. Czink, A. Paier, C. Dumard, T. Zemen, C. F. Mecklenbrauker, and A. F. Molisch, "A geometry-based stochastic MIMO model for vehicle-to-vehicle communications," *IEEE Trans. Wireless Commun.*, vol. 8, no. 7, pp. 3646–3657, Jul. 2009.
[14] A. G. Zajic and G. L. Stuber, "Three-dimensional modeling, simulation, and capacity analysis of space–time correlated mobile-to-mobile channels," *IEEE Trans. Veh. Technol.*, vol. 57, no. 4, pp. 2042–2054, Jul. 2008.
[15] M. Patzold, B. O. Hogstad, and N. Youssef, "Modeling, analysis, and simulation of MIMO mobile-to-mobile fading channels," *IEEE Trans. Wireless Commun.*, vol. 7, no. 2, pp. 510–520, Feb. 2008.
[16] A. G. Zajic, G. L. Stuber, T. G. Pratt, and S. Nguyen, "Wideband MIMO mobile-to-mobile channels: Geometry-based statistical modeling with experimental verification," *IEEE Trans. Veh. Technol.*, vol. 58, no. 2, pp. 517–534, Feb. 2009.
[17] I. Sen, "5 GHz channel characterization for airport surface areas and vehicle–vehicle communication systems," Ph.D. dissertation, School Elect. Eng. Comput. Sci., Ohio Univ., Oxford, OH, Aug. 2007.
[18] D. W. Matolak, I. Sen, and W. Xiong, "On the generation of multivariate Weibull random variates," *IET Commun.*, vol. 2, no. 4, pp. 523–527, Apr. 2008.
[19] L. Cheng, B. E. Henty, D. D. Stancil, F. Bai, and P. Mudalige, "Mobile vehicle-to-vehicle narrow-band channel measurement and characterization of the 5.9 GHz dedicated short range communication (DSRC) frequency band," *IEEE J. Sel. Areas Commun.*, vol. 25, no. 8, pp. 1501–1516, Oct. 2007.
[20] D. Gesbert, H. Bolcskei, D. A. Gore, and A. J. Paulraj, "Outdoor MIMO wireless channels: Models and performance prediction," *IEEE Trans. Commun.*, vol. 50, no. 12, pp. 1926–1934, Dec. 2002.
[21] I. Sen, D. W. Matolak, and W. Xiong, "Wireless channels that exhibit 'worse than Rayleigh' fading: Analytical and measurement results," in *Proc. MILCOM*, Washington, DC, Oct. 23–25, 2006, pp. 1–7.
[22] M. D. Yacoub, "The $\alpha-\mu$ distribution: A physical fading model for the Stacy distribution," *IEEE Trans. Veh. Technol.*, vol. 56, no. 1, pp. 27–34, Jan. 2007.
[23] A. F. Molisch, F. Tufvesson, J. Karedal, and C. Mecklenbrauker, "Propagation aspects of vehicle-to-vehicle communications—An overview," in *Proc. IEEE Radio Wireless Symp.*, San Diego, CA, Jan. 18–22, 2009, pp. 179–182.
[24] R. J. C. Bultitude, "Estimating frequency correlation functions from propagation measurements on fading channels: A critical review," *IEEE J. Sel. Areas Commun.*, vol. 20, no. 6, pp. 1133–1143, Aug. 2002.

Performance Analysis and Computational Complexity Comparison of Sequence Detection Receivers With No Explicit Channel Estimation

Mingwei Wu, *Student Member, IEEE*, and Pooi Yuen Kam, *Fellow, IEEE*

***Abstract*—We consider a single-input–multiple-output (SIMO) fading channel that can be assumed static over a duration of L symbols. We show that the generalized likelihood ratio test (GLRT) receiver for detecting a block of L uncoded symbols does not require channel-state information (CSI). By deriving an exact closed-form pairwise error probability expression for the detector over slowly time-varying Rayleigh fading, we show that its performance approaches that of coherent detection with perfect CSI when L becomes large. To detect a very long sequence of S symbols over a channel that can be assumed to remain static only over L symbols, where $S \gg L$, while keeping computational complexity low, we consider three pilot-based algorithms, namely, the trellis search algorithm, pilot-symbol-assisted block detection, and decision-aided block detection. We compare them with the two existing block-by-block detection algorithms, namely, lattice decoding and sphere decoding, and show the former's advantages in complexity and performance.**

***Index Terms*—Channel-state information (CSI), decision-aided block detection (DABD), fading channels, lattice decoding, pilot-symbol-assisted block detection (PSABD), sequence detection, sphere decoding, trellis search.**

I. Introduction

A signal transmitted over a wireless channel is perturbed by an unknown complex fading gain in addition to additive white Gaussian noise (AWGN). Phase-locked loop (PLL) based coherent detection requires long acquisition times and, therefore, is not suitable for channels with significant time variations or for burst-mode transmission. Differential encoding and differential detection is a viable alternative that does not require explicit channel state information (CSI). However, it incurs substantial performance loss compared with coherent detection. For example, the performance of binary differential phase-shift keying (PSK) is 3 dB worse than that of coherent binary PSK (BPSK) over Rayleigh fading [1]. Joint data-sequence detection and (blind) channel estimation is one approach for designing a coherent receiver. The channel is assumed to remain static over L symbol intervals. We showed in [2] that this approach works well with joint data-sequence detection and carrier phase estimation on a phase noncoherent AWGN channel. We extend this approach here to single-input–multiple-output (SIMO) fading channels and obtain the maximum-likelihood sequence detector with no CSI (MLSD-NCSI) for quadrature-amplitude-modulated (QAM) signals with diversity reception. It is also known as the generalized likelihood ratio test (GLRT) detector [3]. MLSD-NCSI does not require explicit channel estimation or knowledge of the channel statistics in making the data-sequence decision. Multiple-symbol differential detection (MSDD)

Manuscript received December 20, 2008; revised August 5, 2009 and December 22, 2009; accepted February 12, 2010. Date of publication March 18, 2010; date of current version June 16, 2010. This work was supported by the Singapore Ministry of Education Academic Research Fund Tier 2 under Grant T206B2101. The review of this paper was coordinated by Prof. H. H. Nguyen.

The authors are with the Department of Electrical and Computer Engineering, National University of Singapore, Singapore 117576 (e-mail: wumingwei@nus.edu.sg; elekampy@nus.edu.sg).

Color versions of one or more of the figures in this paper are available online at http://ieeexplore.ieee.org.
Digital Object Identifier 10.1109/TVT.2010.2045907